The Structure of River Turbulence

AUTHOR(S):

YOKOSI, Shoitiro

CITATION:

YOKOSI, Shoitiro. The Structure of River Turbulence. Bulletin of the Disaster Prevention Research Institute 1967, 17(2): 1-29

ISSUE DATE:

1967-10

URL:

http://hdl.handle.net/2433/124737

Bull. Disas. Prev. Res. Inst. Kyoto Univ., Vol. 17. Part 2, No. 121, October, 1967

The Structure of River Turbulence

By Shōitirō YOKOSI

(Manuscript received Aug. 10, 1967)

Synopsis

The turbulent velocity of river flow has not been able to be measured accurately because of the lack of a suitable instrument. This paper describes the results of measurements with propeller-type current meters in the Uji river and the Sosui canal.

The turbulence structure of river flow may be characterized by three different scales: width of channel B, horizontally, water depth H, vertically, and furthermore the smallest eddies or Kolmogorov microscale λ_0. It seems to be expedient to split the spectrum into three regions, because $B \gg H \gg \lambda_0$ in a river channel generally. The turbulence characterized by B is large in scale horizontally and quasi-two-dimensional. On the other hand, the turbulence characterized by H is the same as that of usual boundary layer turbulence except in the neighbourhood of a water surface and is three-dimensional.

Interesting results obtained from analyses of observed data are as follows. (1) The energy spectral density is described by the well known 'Kolmogorov $-5/3$ power law' in both horizontal and vertical turbulence. The values of energy dissipation density which is the only parameter determining properties of the inertial subrange are $\varepsilon_H \sim 10^{-2} \mathrm{cm}^2/\mathrm{sec}^3$ for horizontal turbulence and $\varepsilon_V \sim 10^{-1} \mathrm{cm}^2/\mathrm{sec}^3$ for vertical turbulence. (2) The largest eddies of the horizontal turbulence, caused not by an artificial or natural variation of discharge but by the geomorphological features of the river channel itself, is of the order of 10 times the width of the channel longitudinally, and equal to its width laterally. On the other hand, the length of the largest eddies of the vertical turbulence is about 10 times the depth of flow and the width is about 1/10 times of its length. The size of the smallest eddies or Kolmogorov microscale is a little less than 1 mm and most of the turbulence energy comes to be dissipated in the eddies smaller than those of 1 cm in diameter. (3) In the vertical turbulence, turbulence properties near the bottom are very similar to that of well known wall turbulence. However the intersection region formed between a side wall and free surface or bottom has very complicated properties of turbulence.

1. Introduction

In general, river flow is in a state of turbulence. There is little information about turbulence in an open channel flow, although a great deal of knowledge of a mean flow has been obtained in the field of hydraulics. The reasons for this are assumed to be the lack of development of suitable instruments for measuring the turbulent velocity accurately and of serious requirements for studying the internal structure of flow. At present, problems of hydraulics related to turbulence are approached by analogy from the turbulence in the atmosphere, wind tunnel or ocean about which there is a great deal of knowledge[1]. However there is no strong proof that river turbulence is similar to turbulence in other fields. Therefore it seems to be impossible to solve the problems of river turbulence resulting from the characteristic boundary condi-

tions of river flow by the direct analogy with turbulence in other fields. The most necessary thing to do at present seems to be to accumulate extensive knowledge of river turbulence from a large number of observations. This is useful in order to throw light on the turbulence structure of river flow in itself and some time later, can be related to an investigation of mass transport or diffusion phenomena in river flow.

From the above viewpoint, fundamental observations of turbulent velocity were made using the miniature propeller-type current meter and the ordinary electric propeller-type current meter commercially available. The propeller-type current meter is generally simple in construction and easy to deal with, moreover linearity exists between the velocity and revolution of the propeller. The defects are low response and the impossibility of measuring the perpendicular components of the main flow. This type of current meter was supposed to be used originally to estimate mean velocity from the measurement of a long time interval. Therefore turbulence measurement by the propeller type current meter may be not pertinent. However trouble may be removed by appropriate measuring management with the understanding of the limit of application.

Recently in foreign countries, measurements of water turbulence using the propeller-type current meter have been also mentioned[2,3]. A hot-film flowmeter is also used for measuring high frequency fluctuations of velocity, but it has many defects such as difficulty of stable operation and low linearity[4,5]. An electromagnetic flowmeter seems to be inappropriate for turbulence measurement because of its configuration of sensor[6]. The use of an ultrasonic flowmeter which is now considered to have bright prospects has been started in our laboratory[7].

In section 2, the general aspect of river turbulence is presented. Because of the large ratio of width of flow to depth, the velocity field of river turbulence is divided into three regions: quasi-two-dimensional horizontal turbulence, three dimensional boundary layer turbulence and the transitional region between the two. In section 3, results of measurements of turbulence spectra are presented with consideration of turbulence energy dissipation. In sections 4 and 5, shapes of the largest eddies in horizontal and boundary layer turbulence are discussed using cross spectral analysis and moving average. In section 6, several turbulence properties of a boundary layer developed from the bottom and in the corner region between a side wall and a free surface.

These observations were carried out in the Sosui canal running from Lake Biwa to Kyoto and the Uji river. The results obtained are limited to the longitudinal component of flow. However they show a number of interesting facts about river turbulence.

2. General aspect of river turbulence

It can be stated that river flow is one of the irreversible processes of energy transfer. That is to say, potential energy supplied as a precipitation transformed to the energy of mean flow by the gravity force, and the energy supplied continuously to the largest eddies, whose size is of the order of the characteristic dimension of the flow, from the mean flow by the cause of instability is transfered through a cascade of eddies of diminishing size to end in dissipation in

the smallest eddies. Under the equilibrium condition of such energy processes, river flow passes through a river channel and pours into the sea or ocean. On the way, there exist many interesting phenomena in the field not only of natural science but also of engineering : sediment transport, diffusion of suspended materials, meandering of channel, and so on.

For very large Reynolds numbers, eddies of every size from the largest to the smallest are present. An important part in any turbulent flow is played by the largest eddies, whose size is of the order of the dimension of the region in which the flow takes place. These large eddies have the largest amplitudes. If λ is the order of magnitude of the size of a given eddy and v_λ the order of magnitude of its velocity, the turbulence Reynolds number is defined as

$$R_\lambda = \frac{v_\lambda \cdot \lambda}{\nu}. \tag{2·1}$$

The smaller this number is, the smaller the size of the eddy. For a large Reynolds number in the usual sense, the turbulence Reynolds number is also large. Large Reynolds numbers are equivalent to small viscosity. It follows from this that there is no appreciable dissipation of energy in the large eddies. Energy dissipation occurs only with the smallest eddies, whose turbulence Reynolds number is comparable with unity. From the above conception of energy dissipation, the order of magnitude of energy dissipation is determined by the dimensional arguments. The result is that the dissipation of energy is proportional to the third power of the velocity of the largest eddies and inversely proportional to the size of the largest eddies.

In the region which is called the inertial subrange, in which no production and no dissipation take place, the mean energy dissipation ε may be assumed as the energy flux which continuously passes from larger to smaller eddies. Hence the order of magnitude of the turbulent velocity fluctuation v_λ is expressed as

$$v_\lambda \sim (\varepsilon\lambda)^{1/3}, \tag{2·2}$$

from the dimensional argument (Kolmogorov's law). This is a very important result and is equivalent to the well known expression for the energy spectral density

$$E(k) = A\varepsilon^{2/3}k^{-5/3}, \tag{2·3}$$

where k is the wave number related to the size of the eddies as $k=2\pi/\lambda$ and A is the universal dimensionless constant, ε the mean dissipation of turbulence energy per unit time per unit mass of fluid. This relation is valid regardless of the kind of fluid in the region of the inertial subrange : a region much smaller than the size of the largest eddies and much larger than the size of the smallest eddies. Needless to say this relation holds in river turbulence. It will become evident that the assumption that energy flux ε remains constant in a specific region of the spectrum of turbulence, is an important feature of the outline here considered of the turbulent motions of a fluid. There may obviously be turbulent motions in which this condition is not satisfied and where the energy supply is not derived solely from the long wave region of the spectrum, but in

general, from the whole range of wave numbers. For example, river turbulence derives some of their energy from the meandering of flow, wake of pier, sand waves on the bottom, and so on. The size of the eddies produced by the above causes are of the order of magnitude of the size of the causes.

Stationary turbulence rarely exists when the ratio of the size of the largest eddies to that of the smallest eddies increases. As a result, energy dissipation ε must be written not as a constant but as a fluctuating quantity. Recently theoretical studies of the problem have been made[8].

River flow is restricted by the free surface and movable bottom vertically, and by the width of channel horizontally. River flow is usually characterized by a large ratio of width to water depth, which seems to be the essential difference between river turbulence and turbulence in a laboratory flume. The depth H and the width B of river flow are of the order of 10^2 cm and 10^4 cm, respectively, in Japan. Therefore the Reynolds number of river flow is about 10^8 with the depth as a typical dimension and 10^9 with the width. On the other hand, the size of the smallest eddies or Kolmogorov microscale λ_0 is estimated in section 3 as being of the order of 10^{-1} cm by the following expression,

$$\lambda_0=\nu^{3/4}\cdot\varepsilon^{1/4}, \tag{2·4}$$

where ν is the kinematic viscosity and ε the parameter of the mean energy dissipation per unit time per unit mass of water. Therefore the range of the spectrum of river turbulence in the horizontal direction is $B/\lambda_0=10^5$ and in the vertical direction $H/\lambda_0=10^3$. The characteristic size of the eddies in river flow may be expected to be of the order of $\lambda_0=10^{-1}$, $H=10^2$ and $B=10^4$ in cm. The relatively large differences between these three values seem to suggest that it is expedient to split the range of the spectrum of river turbulence into three regions: the regions of $\lambda_0\sim$H, H$\sim$B and an intermediate transitional region. It is well known that the ratio of the size of the largest eddies to the smallest eddies is proportional to the Reynolds number to the power 3/4. If there are no sand waves, no obstacles and no meander in a river channel, in each region, there exists the so-called inertial subrange, in which no production and no dissipation of energy take place and only energy transfer to smaller and smaller eddies occurs because of the sufficiently large Reynolds number of the river flow.

In the region between λ_0 and H in the spectrum of river turbulence, the turbulence, is three-dimensional and characterized by the vertical scale H, because it is quite similar to that in an ordinary turbulent boundary layer except near a free surface. On the other hand, turbulence in the region between H and B is quasi-two-dimensional and characterized by the horizontal scale B. The former would be called 'boundary layer turbulence' or 'vertical turbulence' and the latter 'horizontal turbulence'. The eddies having the lowest wave number in each region of the spectrum correspond to the so-called largest eddies. Therefore the value of energy dissipation ε will be different in vertical turbulence and horizontal turbulence. The statistical properties of turbulence are assumed to be independent in vertical and horizontal turbulence.

The energy transfer in the region of horizontal turbulence is in the state of a cascade process with ε_H and it is supposed that energy may be transmitted to vertical turbulence through the transitional region by the action of turbulent

viscosity

$$\nu_T \sim \varepsilon_H^{1/3} H^{4/3}. \tag{2·5}$$

Energy transmitted from horizontal turbulence to vertical turbulence is transfered to smaller and smaller eddies by a cascade process with ε_ν and, at last, converted by the action of the viscosity ν into heat.

Horizontal turbulence contributes dominantly to, for example, the horizontal and large scale of mixing of suspended or floating matter, because the scale of turbulence is very much larger horizontally than that of vertical turbulence. In the transitional region between the spectra of vertical and horizontal turbulence, the mechanism of energy transfer is very complicated. The turbulence motion of the scale of the largest eddies of vertical turbulence seems to contribute essentially to the dynamic behaviour of river flow on the scale of the order of the water depth, and seems to correspond to a dominant circulation with a diameter of the order of depth around a longitudinal axis and to the streets of spots or voils observed on the surface of a river. These phenomena can be seen in flow patterns over the entire surface of a river obtained from aerial photographs using the Cameron effect[9].

The Reynolds number of river flow and then the width of the spectrum is very large as mentioned above, however it is by far the smaller compared to oceanic or atmospheric turbulence which is in motion on a global scale[10,11].

3. The spectral structure of river turbulence

It is well known that there exist eddies of every size in river flow, but there is little knowledge about the distribution of eddies. The results obtained from the measurement of the velocity field of river turbulence which has a spectrum of wide spread, by a specific measuring instrument are cut at the frequencies corresponding to the size or inertia of the instrument and duration of observation. Therefore, in order to know the structure of river turbulence correctly, pertinent measurement and treatment of data should be made with the understanding of the spread of spectrum in a flow.

Moving average is one of the simple methods of estimating the distribution of the eddies and the size of the largest eddies in a flow. To investigate the dependence of turbulent velocity on the averaging period T_0 it is reasonable to proceed as follows. The dependence is equivalent to the relation between the size and the velocity of the eddies. Let velocity at some point in the river be represented by the function $u(t)$. This function is represented by a superposition of simple harmonic vibration with different amplitude and periods T. When some particular considerations induce selection of an averaging period T, we thereby classify all components with periods greater than T_0 as conforming to a law for the variation of the mean velocity $\bar{u}(t)$ and all velocity fluctuations of higher frequency will then be regarded as turbulent fluctuations $u'(t)$. In order to isolate periods greater than T_0 in a given curve from the other fluctuations the function $u(t)$ must obviously be passed through some selected filter. In the practical application of the smoothing operation to experimental data, it is difficult to employ an ideal filter in most cases. Although the spectral smoothing

characteristic is more or less interior to the ideal filter, we use smoothing of the following form,

$$\bar{u}_k = \frac{1}{T_0} \sum_{i=k-\frac{T_0}{2}}^{k+\frac{T_0}{2}} \left[1+\cos\frac{2\pi(k-i)}{T_0}\right] u_i. \tag{3·1}$$

Having derived the averaged function $\bar{u}(t)$, we easily obtain the corresponding fluctuating velocity $u'(t)$. We can also analyze the value of $\overline{u'^2}$ as T_0 increases. It is easily seen that this is the energy of the longitudinal turbulent fluctuations having periods smaller than T_0. If smoothing is performed with an entire set of the smoothing parameter T_0, we can then generally obtain the energy distribution. In other words, this method can be used to investigate the energy spectrum of the turbulent fluctuations of river velocity.

As mentioned already, various sizes of eddies are distributed widely in river flow. The spectral representation seems to be the most useful for this problem. According to the modern theory of turbulence, energy flux or energy dissipation ε is the only determining parameter of all the statistical properties of turbulence in the region of the range of local isotropy. The form of the energy spectral density has been determined theoretically in this region. It is well known as the Kolmogorov $-5/3$ power law, and numerous experiments have justified this theory. The one-dimensional spectrum function $F(n)$ is expressed in terms of the frequency from the three-dimensional spectrum function (2·3) as follows,

$$F(n) = \frac{C}{(2\pi)^{2/3}} \bar{u}^{2/3} \varepsilon^{2/3} n^{-5/3}, \tag{3·2}$$

where C is the universal dimensionless constant and $C=(9/55)A$[1], n the frequency (1/sec), $\bar{u}$ the mean velocity at a given point (cm/sec), ε the energy dissipation per unit time per unit mass (cm^2/sec^3). The most recent determinations suggest that C is between 0.45 and 0.51[1]. Grant *et al.*[5] have obtained a value for C of 0.47 ± 0.02, in the case of water turbulence in a tidal channel; the viscous dissipation rates ranged from 0.0015 to 1.02 cm^2/sec^3. The experimental value of the constant C has recently been verified theoretically by R. H. Kraichnan[12].

The energy flux ε is a very important parameter as mentioned already. There exist a large number of estimates of the dissipation ε in the field of atmospheric turbulence[1]. It is simple to determine the $u_*^2(d\bar{u}/dz)$, where u_* is friction velocity. This is the rate of production of mechanical energy, under conditions when turbulent energy is in equilibrium, and near the boundary wall all the terms in the energy equation can be neglected except terms of production and dissipation of energy. Diffusion experiment and integration of the spectrum measured in the dissipation range also give the methods of estimation of the value of ε. In this paper, we estimate ε from the expression (3·2) under the assumption of the value of the universal constant C.

The most comprehensive practical procedure to give a spectrum is as follows. The method is intended to provide a realistic analysis of a finite series of discrete observations such as would be obtained by reading a velocity record at

prescribed intervals. With N observations at intervals of time Δt the first step is to form the auto-correlation function R_k of the values u_i $(i=1, 2, \ldots, N)$ for successive values of lag $k\Delta t$,

$$R_k=\frac{1}{N-k}\left[\sum_{i=1}^{N-k}u_iu_{i+k}-\frac{1}{N-k}\sum_{i=1}^{N-k}u_i\sum_{i=1}^{N-k}u_{i+k}\right], \quad (k=0, 1, \ldots, m). \tag{3·3}$$

From the values of auto-correlation function obtained in this manner, power spectral densities are calculated.

$$F_h=2\Delta t\left[R_0+2\sum_{k=1}^{m-1}R_k\cos\frac{kh\pi}{m}+R_m\cos\pi h\right]. \quad (h=0, 1, 2, \ldots, m) \tag{3·4}$$

Each value of F_h corresponding to a frequency band whose mid-point is found by means of the formula:

$$n_h=\frac{h}{2m\Delta t} \tag{3·5}$$

where Δt is the interval between successive observations. To obtain a better spectral estimate than that of (3·4), a simple smoothing operation is performed. In this investigation the Hamming procedure was used and final spectral estimates were obtained.

The choice of the number of lags is important. For resolution of the spectrum into narrow bands m should be as large as possible, but if it is too large the computational work involved may be prohibitive and, more important probably, the accuracy of the estimates decreases. Tukey[13] suggests that m should be small enough in relation to N to make the number of degrees of freedom f satisfactorily large,

$$f=\frac{2(N-m/1)}{m}. \tag{3·6}$$

(a) Observations

Observations of river turbulence were conducted with a propeller-type current meter in the Uji river, Kyoto. The Uji river, flowing in front of our laboratory, rises in Lake Biwa and discharges into Osaka Bay. The observation point at Yodo is about 38 km up the river mouth. There is no tidal influence. The flow is regulated by the Amagase Dam situated about 17 km upstream from Yodo. In the upper 10 km reach from the observation point at Yodo, the river channel has a constant width of about 100 m, and there are no sudden curves and no large amounts of inflow. In the reach shown in the location map in Fig. 3. 1, the channel is repaired regularly so as to be almost constant in width and depth. In this reach the width and depth of the channel are uniformly about 100 m and 4 m, respectively, the bottom is sandy, the slope of the river is 0.00026 and Manning's roughness coefficient is 0.027. It is considered that a statistically stable state of river turbulence is presented. Since the Yodo water gauge is

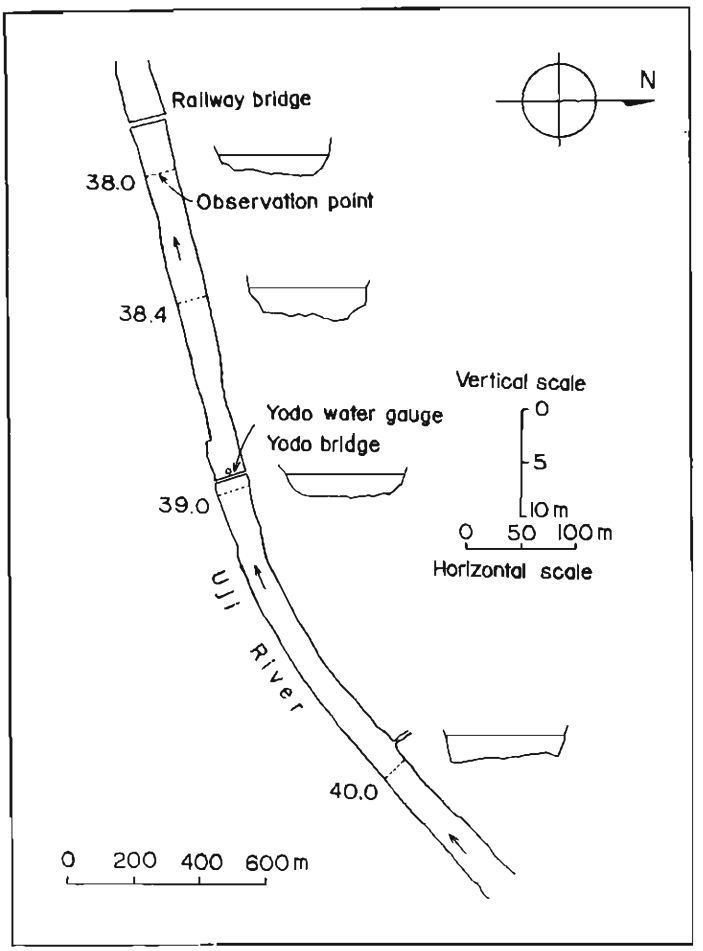

Fig. 3. 1 Location map. Numerals indicate the distance from river mouth in km.

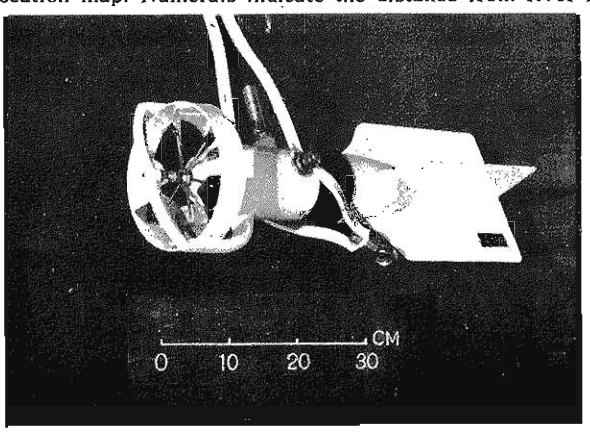

Photo. 3. 1 An electric propeller-type current meter.

conveniently situated about 1 km up from the observation point, variations in the discharge of flow could be checked during the observation.

The measuring instrument used is shown in Photo. 3. 1. It is a commercial six-bladed propeller-type current meter, and the propeller is 14 cm in diameter. The rate of turning of the propeller is linearly proportional to flow speeds normal to the blades and closely follows the cosine function for all other angles of attack. The propeller drives a low-inertia, low-friction DC tachometer generator. Since the generator in its watertight body and the shaft of the propeller are coupled magnetically, the output voltage of the tachometer generator is essentially linearly proportional to the flow speed. This permits the output to be measured by almost any millivolt recorder. The axis of the propeller is always set in the direction of flow by the tail fins mounted on the instrument body. The starting speed of the current meter with the generator engaged is about 10 cm/sec, and the time constant of the whole instrument after connecting with a pen-writing recorder is evaluated to be less than 0.6 sec for frequency response. The recorder used has a 2 MΩ input impedance. Therefore this meter is sufficiently available for measuring the fluctuating velocity in the direction of the mean flow, having frequencies lower than 1 cps.

It is clear that these instruments are not suited for the study of the fine structure of the velocity field or of high frequency fluctuations in the river turbulence spectrum. However, the very large horizontal dimensions of a river result in large scale horizontal processes. Therefore a long series of observations extending over many hours is requried when studying the large scale characteristics of horizontal velocity. The small period fluctuations, which contribute only negligibly to horizontal turbulence, can be neglected altogether. Therefore this current meter can be regarded as entirely satisfactory for investigating the large scale velocity fluctuations that contain a considerable portion of the energy of river turbulence.

During the observations, the current meter was suspended in the center of the channel from a wire rope stretched between the two banks, and the position of the instrument was 40 cm below the surface of water for convenience of observation. The fluctuating velocities were recorded by the self-balancing type of pen-writing recorder taken on a motor boat anchored a few meters down from the current meter.

(b) Moving averaging

In May of 1966, an observation of turbulent velocity was made during a period of 30 min. The depth of water was 2.0 m and the average velocity over 30 min was 1.28m/sec. The smoothing procedures were carried out on the data obtained from the 30 min observation. The amplitudes of the fluctuations of velocity were read off at 0.6 sec intervals, which were then subjected to smoothing using formula (3·1) and $T_0=1.2$, 6.0, 60 and 300 sec. Fig. 3. 2 shows graphically how an increase of the averaging period causes all the smaller scale fluctuations to disappear, so that the curves become increasingly smoother.

The length of the largest eddies of the vertical turbulence is assumed to be nearly equal to 10 times the height from the bottom, and then their passage time $10\,H/\bar{u}$ is about 1/4 min in this case. These eddies are clearly contained in the result with the averaging period of 6 sec. Existence of a great variety of eddies

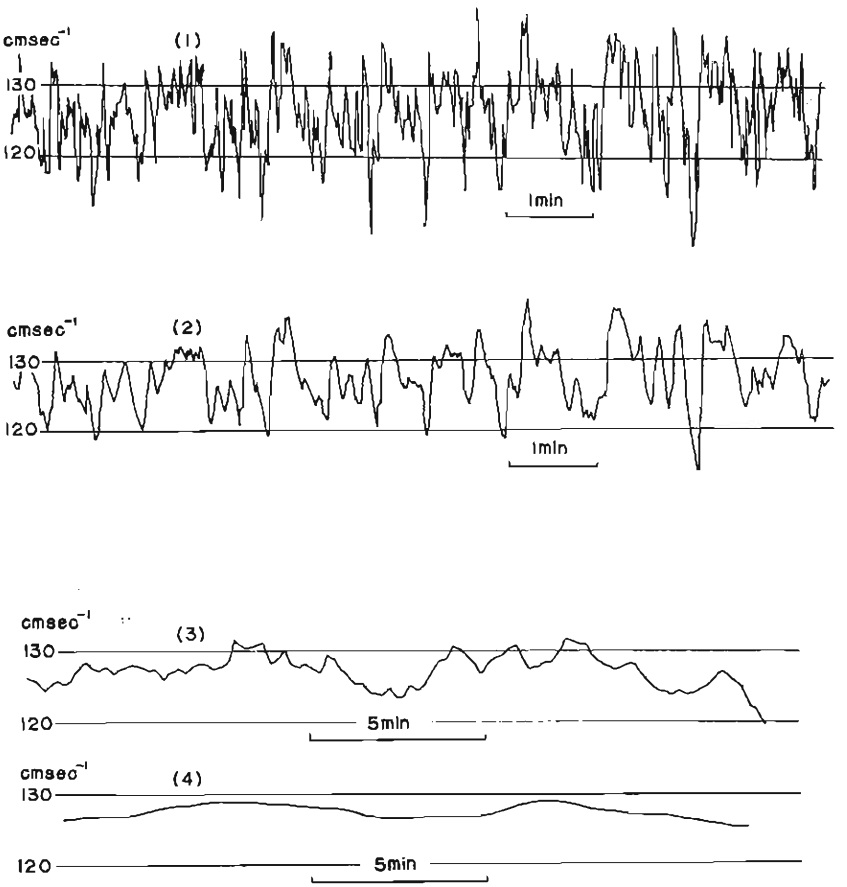

Fig. 3. 2 Velocity Variations in the river for different averaging periods. (1) : Instantaneous values, (2) : with the averaging period 6 sec, (3) : 1 min, (4) : 5 min. $B=100$ m, $H=2.0$ m, $\bar{u}=1.28$ m/sec.

larger than these is also seen in Fig. 3. 2. We can understand from this figure that the spectrum of turbulent velocity in river flow is wide spread. The result with the averaging period of 5 min awakens our interest because there seems to be a long wave with a period of about 10 min, although only one wave exists. The length of this eddy is estimated to be nearly equal to 10 times the width of the channel using the frozen turbulence hypothesis. This will be refered to in section 4 in detail.

(c) Power spectrum

In order to obtain the whole figure of the spectrum of river turbulence, the observation of turbulent velocity was conducted during a period of 1 hour with the propeller-type current meter at Yodo in September of 1966. The location of observation and the instrument used were mentioned above. During the observation, depth of water was 2.7 m and averaged velocity during 1 hour was 1.3m/sec. A root mean square value of the velocity fluctuation $\sqrt{\overline{u'^2}}$ during 1 hour

was estimated as 6.62 cm/sec, and then turbulence intensity was $\sqrt{\overline{u'^2}}/\bar{u}=0.051$. The root mean square value during 1 hour is assumed to be nearly equal to the velocity of the largest eddies of the horizontal turbulence in this case. The reason is as follows. The duration of 1 hour is larger than the passage time of the largest eddies of the horizontal turbulence, and then the value $\sqrt{\overline{u'^2}}$ during 1 hour contains the root mean square value of the largest eddies of the horizontal turbulence. Moreover, if the velocity fluctuations of horizontal and vertical turbulence are represented as $u_H(t)$ and $u_V(t)$, respectively, total fluctuation of river turbulent velocity is expressed by

$$u(t)=u_H(t)+u_V(t). \tag{3·7}$$

Therefore if $u_H(t)$ and $u_V(t)$ are statistically independent,

$$\overline{u'^2(t)}=\overline{u_H'^2(t)}+\overline{u_V'^2(t)}. \tag{3·8}$$

Hence the following relation is obtained because $\sqrt{\overline{u_H'^2}}\gg\sqrt{\overline{u_V'^2}}$,

$$\sqrt{\overline{u'^2}(t)}\simeq\sqrt{\overline{u_H'^2}(t)}. \tag{3·9}$$

The energy spectral densities calculated by the formulae (3.3), (3.4) are shown

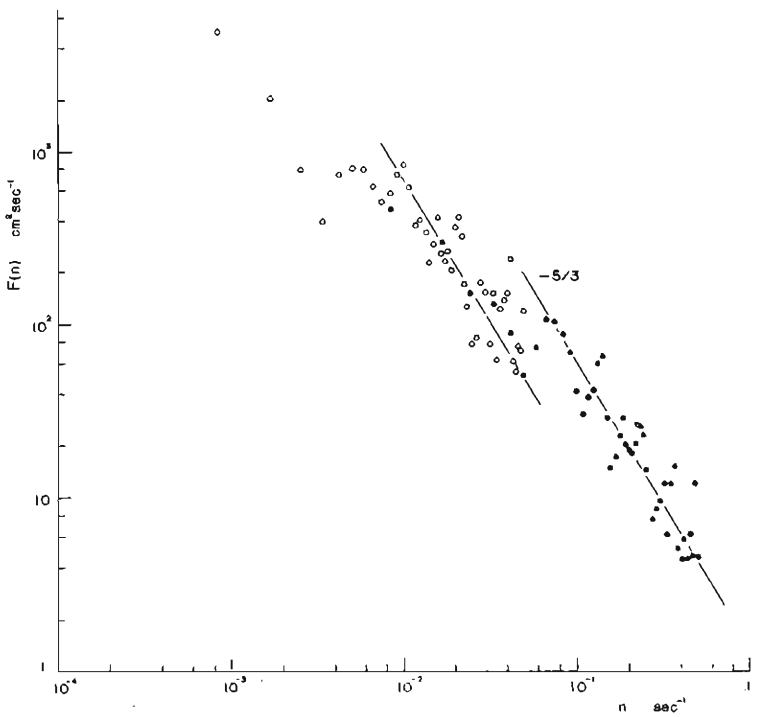

Fig. 3. 3 Energy spectral density of the longitudinal velocity in the river. $B=100$ m, $H=2.7$ m, $\bar{u}=1.30$ m/sec.

in Fig. 3. 3. In this figure, black and white circles represent the values estimated from the data which was obtained by applying the moving average of a period of $\Delta t=1$ sec and $\Delta t=10$ sec to the original data. This procedure was carried out for convenience of computation. The energy densities obtained from the average were corrected with the aid of the weighting function $\sin^2\pi n\Delta t/(\pi n\Delta t)^2$.[14]

The energy densities distribution is in good agreement with the Kolmogorov $-5/3$ power law in both the region of horizontal and vertical turbulence. However the parameter of the mean energy dissipation which is the only parameter describing the statistical characteristics of the inertial subrange is different in each region. There exists a transitional region between the frequencies 0.05–0.06 cps, which corresponds to the frequency of passing of the largest eddies of the vertical turbulence at the observation point. It has been already found that their length is nearly equal to 10 times the height from the bottom.[15]

The parameters of the mean energy dissipation were estimated from Fig. 3. 3 and Eq. (3·2) as $\varepsilon_H=0.030\,\mathrm{cm^2/sec^3}$ for the horizontal turbulence and $\varepsilon_V=0.21\mathrm{cm^2/sec^3}$ for the vertical turbulence. In this estimation, the universal constant C in Eq. (3·2) was chosen as 0.50. The value of ε permits the estimation of the Kolmogorov microscale λ_0 from Eq. (2·4), and this scale is nearly equal to the size of the eddies of maximum dissipation[16]. The results are that $(\nu^3/\varepsilon_H)^{1/4}=0.076$ cm in a low frequency range and $(\nu^3/\varepsilon_V)^{1/4}=0.047$ cm in high frequency range. Most turbulence energy comes to be dissipated in eddies smaller than those of 1 cm in diameter, because MacCready[16] says that 90% of viscous dissipation occurs in the eddies smaller than those of 15 times of the microscale of Kolmogorov. On the other hand, turbulent viscosity that transmits energy from horizontal turbulence to vertical turbulence through the transitional region was evaluated as $8.7\times10^3\,\mathrm{cm^2/sec}$ from Eq. (2·5).

A similar observation was made in the same month at the same place. The condition of the observation was that water depth at the observation point was 2.7 m and the position of the current meter was 40 cm below the surface in the center of the channel. Fig. 3. 4 shows the estimated spectral distribution. The average velocity during 1 hour was 144 cm/sec and the root mean square value of the velocity fluctuation was 7.2 cm/sec. This spectrum is presented in a different way from that in Fig. 3. 3. Plotting $nF(n)$ against $\log n$ gives a form of spectrum curve which is much used in practice, for while using a scale which is more convenient when large ranges of frequency are involved, it retains the useful feature of representing the contribution to the total variance in specified frequency bands, since $nF(n)d(\log n)=F(n)dn$. The nondimensional frequency $nH/\bar{u}$ used in the figure may be regarded as the ratio of the depth to the wavelength. The significant feature of the spectrum is the presence of the vertical turbulence maximum which lies at $nH/\bar{u}=0.1$. That is to say, the length of the largest eddies of vertical turbulence is about 10 times the depth. In order to know the statistical properties of the horizontal turbulence maximum, duration of observation should be at least 10 times the passage time of the horizontal largest eddies. This problem will be referred to in the next section.

Fig. 3. 4 shows that there exists a gap between the horizontal and vertical turbulence regions. Such a gap in the spectrum is well known in atmospheric turbulence[1], but much wider and deeper than that in Fig. 3. 4. That is to say,

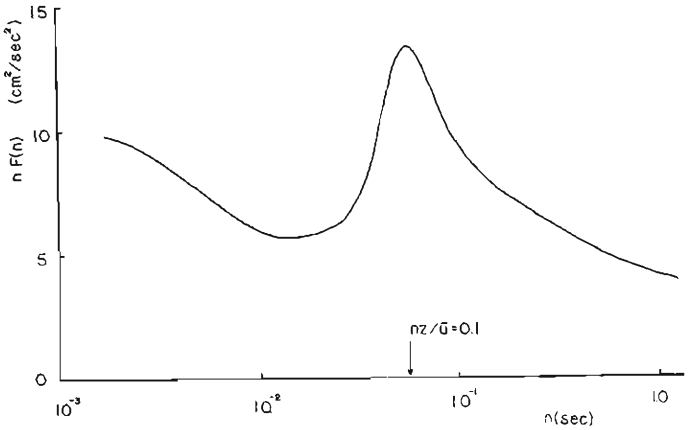

Fig. 3. 4 Schematic spectrum of longitudinal velocity in a river.
$B=100$ m, $H=2.7$ m, $\bar{u}=1.44$m/sec.

there exist a synoptic maximum of approximately 4 days, a micrometeorological maximum of the order of 1 min and a wide mesometeorological minimum separating them in intervals of several minutes up to several hours. The actual separation of the synoptic and micrometeorological fluctuations substantially mitigates the difficulties in determining the mean values of the micrometeorological characteristics connected with the phenomenon of the evolution of the level of the meteorological fields. If the gap in the spectrum of river turbulence is very wide, it permits a relative determination of the stable mean values by the averaging by periods which belong to the region of the trasitional region of the spectrum. However, the gap in the spectrum of river turbulence is unfortunately not so large.

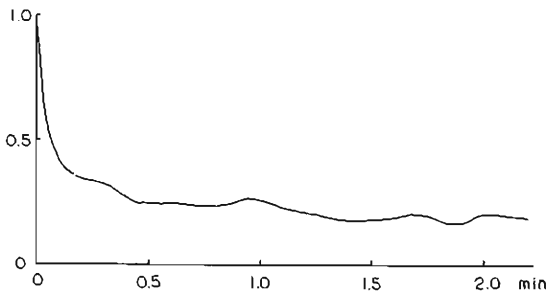

Fig. 3. 5 Auto-correlation coefficient of turbulent velocity of river flow.
$B=100$ m, $H=2.7$ m, $\bar{u}=1.44$ m/sec.

The correlogram calculated before the spectrum of Fig. 3. 4 is shown in Fig. 3. 5. This closely resembles the auto-correlation function of the sum of two statistically independent stationary random processes of markedly different scales[17]. This also shows the adequacy of splitting the spectrum of river turbulence into regions of horizontal and vertical turbulence.

As mentioned already, there exist two characteristic scales of width and depth in the simple straight open channel of large width. However in a real river, there exist many characteristic scales which are of the order of magnitude of the size of eddies related to the turbulence energy input, such as the eddies produced by the meander of channel, bottom roughness, hydraulic structures, and so on. An actual figure of the field of the river turbulence will be a superposition of all these effects.

A similar figure of the velocity field is proposed by Ozmidov[10] in oceanic turbulence, where the energy supply to oceanic turbulence occurs around the scale of wind waves, of inertial and tidal oscillations, and in the scale range of major atmospheric disturbances.

4. The largest eddies of horizontal turbulence

The scale of horizontal turbulence is usually so much greater than the vertical scale that its effects can be considered separately. As was pointed out earlier, a very wide spectrum of horizontal turbulent motions exist in a river. The statistical properties of horizontal turbulence are assumed to be nearly uniform in a vertical direction. Therefore we can regard them just as two-dimensional thin 'discs'. It is clear that large scale horizontal mixing due to the horizontal eddies plays an important part in the turbulent diffusion in a river. Between these large 'discs', existence of the cascade process of turbulent energy, that is an applicability of the Kolmogorov $-5/3$ power law has been already shown in Fig. 3. 3.

In order to estimate the size of the largest eddies of horizontal turbulence, observation similar to that mentioned in the foregoing section was carried out. The average velocity during the observation period of 1 hour was 1.23 m/sec and the water depth was 2.1 m. The result obtained by applying the moving average of a period of 5 min to the original record making use of the Eq. (3·1) is shown in Fig. 4. 1.

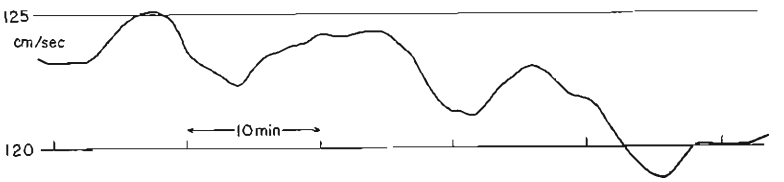

Fig. 4. 1 Velocity variations in the river with the averaging period 5 min. $H=2.1$ m, $\bar{u}=1.23$ m/sec.

Obviously, the dominant period of about 14 min is found in this figure. This period corresponds to that of passage of the eddies whose size is nearly equal to 10 times the width of the flow. It may be assumed that they are the largest eddies of horizontal turbulence, the length of which is about 1 km in this reach of the river, because excessively slender eddies cannot exist stably and the motion of the largest eddies has been assumed to be fairly regular. The gradual decrease of velocity in Fig. 4. 1 is due to the operation of discharge at the Amagase

Dam, which was detected from the record of water level at the Yodo water gauge situated 1 km above the observation point.

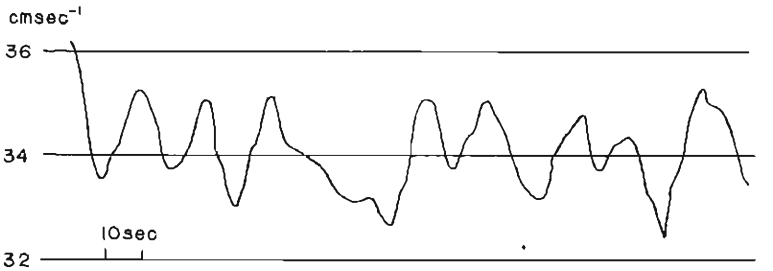

Fig. 4. 2 Velocity variations in the laboratory flume with the averaging period 10 sec. $B=60$ cm, $H=15$ cm, $\bar{u}=34$ cm/sec, length of the flume $=150$ m.

Laboratory experiment concerning the size of the largest eddies also supports the fact just mentioned above. Velocity variation was measured near the end of the experimental flume 150 m long and 0.6 m wide using the miniature propeller-type current meter, the details of which are described in section 6. The water depth was fixed at about 15 cm during measurement. Formation of the stable field of horizontal turbulence is expected from the reach into 150 m. Figure 4. 2 shows the result of the moving average with the averaging period of 10 sec with the use of the formula (3·1). Since the width of the channel B was 60 cm and mean velocity $\bar{u}$ was 34 cm/sec in this experiment, the passage time of the horizontal largest eddies $10B/\bar{u}$ is estimated as about 18 sec. In this figure, the average of the dominant period of velocity variation seems to be approximately 18 sec.

The size of the largest eddies of horizontal turbulence, caused not by the artificial or natural variations of a flow discharge but the geomorphological features of a river channel itself, is assumed to be of the order of 10 times the width of the channel longitudinally, and equal to its width laterally and to the depth of the flow vertically[18]. These facts are very interesting for us considering the fact that the length of the largest eddies of the vertical turbulence is of the order of 10 times the depth of flow. When, therefore, the detailed statistical properties of the horizontal largest eddies are required, observation of the velocity fluctuation during the period of $100B/\bar{u}$ is, at least needed, which is 10 times the passage time of the horizontal largest eddies. But in general, continuous observation of velocity during such a long period is difficult because of the variation in the discharge of flow and because the existence of floating matter disturbs the revolution of the propeller of the current meter.

5. The largest eddies of vertical turbulence

Turbulence energy of horizontal turbulence is transmitted to vertical turbulence through the transitional region. In this process of energy transfer, the transitional region poses a very important problem, where the energy of the two-dimensional field is transmitted to the three-dimensional velocity field. The eddies of the transitional region or the largest eddies of vertical turbulence seem

to correspond to the scale of motions such as dominant circulations of a diameter of the order of the depth and the phenomena of streets of spots or voils observed on the surface of a river.

In order to clarify the statistical properties of the largest eddies of vertical turbulence, observations of turbulent velocities were conducted at Yodo using two propeller-type current meters. The location of observation and the measuring instrument have already been described in detail in section 3. During the observation, the depth of water was 2.7 m and the average velocity during 1 hour was 1.3 m/sec. Therefore the Reynolds number was 3.5×10^6 with the depth and 1.3×10^8 with the width, because the width of the flow was 100m. If Taylor's hypothesis of frozen turbulence is permitted, a longitudinal scale of energy containing eddies or the largest eddies and an average eddy size can be estimated from the velocity measurement with one instrument. However a lateral scale of such eddies cannot be estimated from the observation with one instrument; at least two instruments arranged laterally are necessary for this purpose. During the observation, one current meter was fixed in the center of the channel and the other one was moved laterally with separation distances of 0.5, 1.0, 1.5, 2.0, 3.0, 4.0, 5.0, 7.0 and 10 m. Each current meter was suspended 30 cm below the water surface, and longitudinal velocity fluctuations were measured simultaneously for 5 min at each separate distance.

The amplitudes of the fluctuations in the two traces on each record were read off at 1 sec intervals and from this data the root mean square values, power spectra and cross-spectra for various time lags were computed. The average value of the relative turbulence intensity of the longitudinal velocity fluctuations was 0.057 which was obtained from 18 series of data of 9 sets of observations. The relative height of the current meter to water depth was 0.85. The distribution of the energy spectral densities of 18 series of data is shown in Fig. 5. 1, and the Kolmogorov $-5/3$ power law is also presented. The dissipation of turbulent energy was estimated as $\varepsilon_V=0.74\ \mathrm{cm^2/sec^3}$ from the method used in section 3. This value agrees with that obtained in section 3 in order of magnitude.

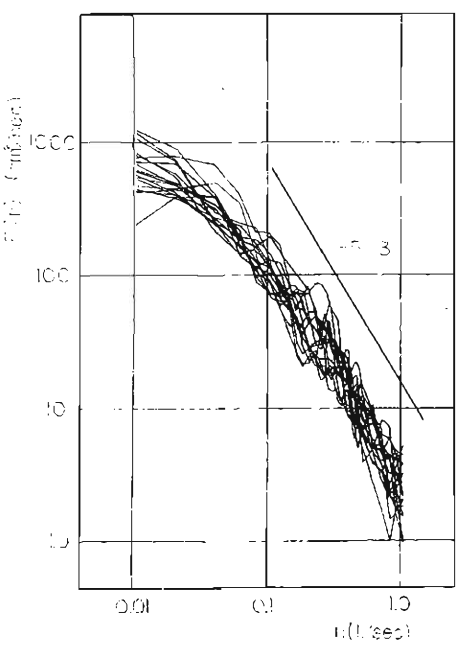

Fig. 5. 1 One dimensional spectral densities of river turbulence. $R=3.5\times10^6$.

The average eddy size or integral scale is obtained from the correlation measurements. In this paper, the longitudinal integral scale L_x was calculated from the longitudinal integral time scale,

$$T_x=\int_0^\infty R_x(t)\,dt, \qquad (5\cdot1)$$

using Taylor's frozen turbulence hypothesis $L_x=\bar{u}T_x$, where $R(t)$ is an autocorrelation coefficient obtained from (3·3) divided by the variance. The result was $L_x=4.8$ m, that is, the average eddy size is twice the height of the observation point. The determination of the integral time scale of vertical turbulence is difficult when the correlations do not come to zero rapidly, because of the existence of trends in the data. The trends are the velocity variation of horizontal turbulence, the periods of which are not so large compared to that of velocity fluctuations of vertical turbulence, because the gap or transitional region of the spectrum is small. On the other hand, the lateral integral scale was obtained from the covariances measured at each separation of instruments. The lateral spatial correlation curve is shown in Fig. 5. 2. The area under the correlation curve gives an indication of an average eddy size in the lateral direction. The result was $L_y=0.95$ m, which was 2/5 times the height of the instruments. After all, the length of the average eddy is about 5 times its width.

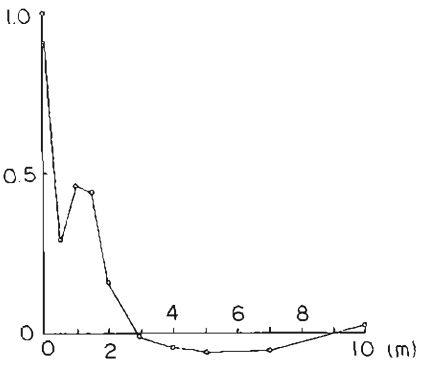

Fig. 5. 2 Lateral spatial correlation.

The length of the largest eddies of vertical turbulence was already estimated as 10 times the height, which is also estimated here as follows. We assume that the large eddy end of the inertial subrange of the spectrum corresponds approximately to the frequencies of the largest eddies. From the turbulence spectra of the longitudinal velocities in Fig. 5. 1, the isotropic limit where the slope of the spectra begins to deviate from that of $-5/3$ seems to lie at about 0.05 cps. The ratio of height to wavelength $nz/\bar{u}$ is then about 0.1. That is to say, the length of the largest eddies of vertical turbulence is nearly equal to 10 times the height.

The width of the largest eddies is determined from the lateral spatial spectrum of turbulence. However there is no data available for the calculation of lateral spatial spectrum of river turbulence so we calculated it from the data obtained from the measurements by two current meters arranged laterally, using the cross-spectral analysis.

From the two series of velocity fluctuations $x(t)$ and $y(t)$ measured at two positions, cross correlation functions are calculated by means of the formulae:

$$R_{xy}(k)=\frac{1}{N-k}\left[\sum_{i=1}^{N-k}x_iy_{i+k}-\frac{1}{N-k}\sum_{i=1}^{N-k}x_i\sum_{i=1}^{N-k}y_{i+k}\right], \tag{5·2}$$

$$R_{yx}(k)=\frac{1}{N-k}\left[\sum_{i=1}^{N-k}x_{i+k}y_i-\frac{1}{N-k}\sum_{i=1}^{N-k}y_i\sum_{i=1}^{N-k}x_{i+k}\right], \tag{5·3}$$

$$(k=0,\ 1,\ \ldots,m),$$

where N is the total amount of data and m is the maximal lag of the correla-

tion function. Cross correlation is not necessarily either even or odd, hence cross spectrum is given by

$$Co(h)=2\Delta t\left[E(0)+2\sum_{k=1}^{m-1}E(k)\cos\frac{kh\pi}{m}+E(m)\cos\pi h\right], \tag{5·4}$$

$$Q(h)=4\Delta t\sum_{k=1}^{m-1}O(k)\sin\frac{kh\pi}{m}, \tag{5·5}$$

where $E(k)$ and $O(k)$ are even and odd parts of cross correlation,

$$E(k)=\frac{1}{2}(R_{xy}(k)+R_{yx}(k)),$$

$$O(k)=\frac{1}{2}(R_{xy}(k)-R_{yx}(k)),$$

and Co is the real part of the cross spectrum, Q the imaginary part. They are called cospectrum and quadrature spectrum respectively. The cospectrum measures the contribution of various frequencies to the covariance. The quadrature spectrum is zero if the cross correlation is even. From the values of Co and Q the so-called coherence Coh is calculated. This is the square of the spectral correlation, that is, the normalized covariance;

$$Coh=\frac{Co^2+Q^2}{F_x\cdot F_y}, \tag{5·6}$$

where F_x and F_y are power spectral densities of $x(t)$ and $y(t)$, respectively. This is the value characterizing the coupling between fluctuations of a given frequency in the two series of observations under consideration. If the fluctuations in both series have a constant phase lag, their coherence is equal to unity. If their phase lag has random values, then for sufficiently long series, the function Coh becomes zero. The phase lag is given by

$$\varphi=\tan^{-1}\frac{Q}{Co}, \tag{5·7}$$

where the unit of φ is a radian.

Fig. 5. 3 shows the coherences and phase lags calculated for each separation of instruments by the formulae (5.2)−(5.7). The results calculated for the separation of instruments larger than 3 m are not presented in this figure, because their coherences were negligible. According to the increase of separations, coherences decrease to zero and phase lags leave from zero at low frequency. Assuming that the coherence decreases linearly in the low frequency region, let the frequency where the coherence becomes zero be n_o, let the separation distance between two instruments be d and the mean velocity $\bar{u}$. The value $n_o d/\bar{u}$ indicates the ratio of the separation distance between two instruments to wavelength. An averaged value of $n_o d/\bar{u}$ calculated from the coherences when the separations were $d=$ 0.5 and 1.0 m was about 0.1. This means that if the separation distance becomes 1/10 of the wavelength, coherences come to zero, that is to say, there

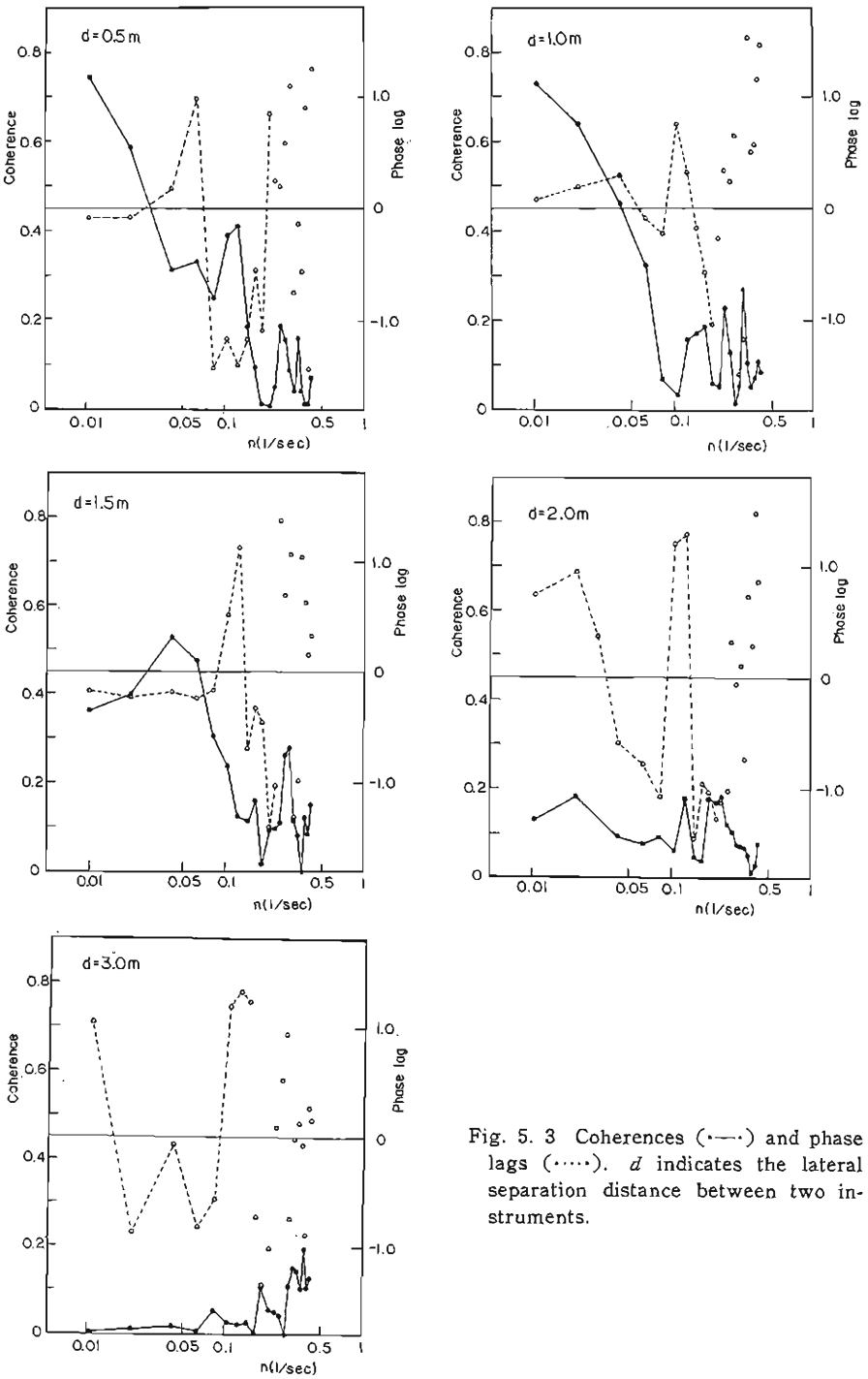

Fig. 5. 3 Coherences (•—•) and phase lags (•·····•). d indicates the lateral separation distance between two instruments.

exists no correlation between the two series of velocity fluctuations. We therefore conclude that the width of the largest eddies of vertical turbulence is about 1/10 the length of these eddies. After all, the size of the largest eddies of vertical turbulence is of the order of 10 times the depth of flow longitudinally and nearly equal to its depth vertically.

The phase lags in the low frequency region were approximately zero at the short separation. According to the increase in frequency, the values of phase lag fluctuate violently plus and minus in a random manner. In this case negative phase lag indicates that the phase of the fluctuation measured by an instrument that is moved lags compared to that measured by a fixed one. It seems to be very important for an understanding of the nature of the largest eddies whether the sign of the phase lag becomes plus or minus from zero in the lowest frequency region. The problems related to the phase lag must be discussed with consideration of the value of coherence, because the phase lag at a frequency where the coherence is very small is meaningless. At this observation, the duration of observation was too short to discuss the coherence and phase lag in detail.

Two other similar observations were conducted after the position of the fixed current meter was changed. Their spatial correlations and coherences were too small to discuss the size of the largest eddies. It was supposed from these results that in uniform river flow there exist rows of secondary circulation with a streamwise axis that are very stable spatially. Therefore the results obtained are different according to the lateral position of the observation. These facts seem to be supported by the flow patterns obtained from the aerial photograph[9].

6. The structure of vertical turbulence

In the vertical turbulence of river flow, contrary to horizontal turbulence, there exists a strong shear of mean flow in the region near a solid boundary. The turbulence structure of the boundary layer developed from a bottom with no effect from a side wall is assumed to be similar to that of usual boundary layer. A turbulence structure near the free surface differs from that of a rigid wall, because tangential and vertical movements are not prohibited at the boundary. Furthermore the stress at the free surface is zero. In the region near a side wall, boundary layers developed from the wall, bottom and free surface interfere with each other and generate a strong secondary flow and complicated turbulence structure. These are the peculiar features of open channel turbulence, in itself distinguished from other fields of turbulence.

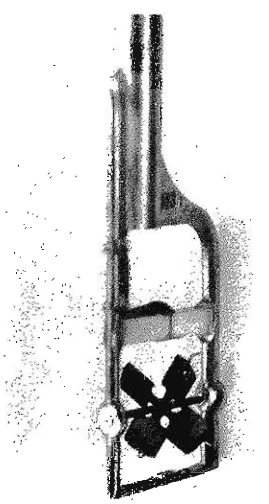

Photo. 6. 1 A miniature propeller-type current meter. The diameter of the propeller is 1.5 cm.

Two kinds of observation of boundary layer turbulence were conducted in the Sosui canal with the use of a miniature propeller-type current meter. The one was of the boundary layer between the bottom and a free surface developed from the bottom, and the other of the corner region consisting of a side wall and a free surface.

(a) Measurements

Turbulent fluctuations of velocity were measured with a miniature propeller-type current meter which consists of a four-bladed propeller 1.5 cm in diameter (Photo. 6. 1). The shaft of the propeller was supported by jewel bearings. When the propeller blades rotate between a pair of platinum electrodes mounted in the frame at right angles to the propeller axis, four electric pulses due to the variation in electric resistance are generated by one rotation of the propeller.

The average velocity U(cm/sec) was represented by the number of pulses per second p as

$$U=0.76p+2.4. \tag{6·1}$$

Starting speed was about 3cm/sec. In order to know the response of the instrument, time constant τ was estimated for various speeds U_o assuming an exponent transient response, which is shown in Fig. 6. 1. A limitation of turbulence measurement with this instrument is clear from this figure. That is to say, since this instrument is not sensitive to the fluctuation of velocity, frequency of which is higher than that of response, the spectrum of phenomena is cut off at this frequency.

The pulses generated by the current meter were recorded continuously by a pen-writing oscillograph through a dynamic strainmeter and DC amplifier. Recorded pulses were counted continuously at 1 sec intervals and velocity calculated from (6·1) was regarded as an average velocity during an averaging time of 1 sec. Since this type of current meter was supposed to be used originally to estimate an average velocity over a long time interval, the procedure which estimate an average velocity during 1 sec from the number of pulses during an averaging time of 1 sec is a question. To be exact, the velocity calculated from p differs from the real velocity because the value of p is represented as an integer in spite of continuous velocity variation. This error decreases relatively when the velocity or averaging time increases. Therefore in using this type of current meter, besides the limitation due to the size and response of the current meter, the limitation due to the indicating mechanism of the rotation of propeller must be taken into consideration. If the error of this type is relatively large,

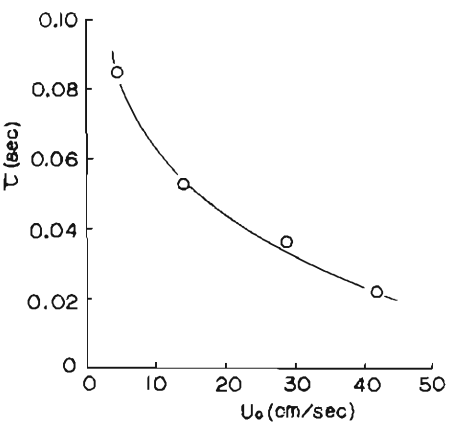

Fig. 6. 1 Dependence of time constant of current meter on velocity.

turbulence properties in the flow will be masked by this error like a white spectrum[15].

The choice of sampling duration is also important. For the observation to determine the statistical properties of vertical turbulence in detail, the irreducible minimum of time for the observation is about 10 times as long as the passage time of the largest eddies or energy containing eddies. That is, the sampling duration needed is at least $100z/\bar{u}$, where z is the distance from the wall and $\bar{u}$ the mean velocity at this distance. However, a needlessly long time of observation would be in danger of entering unwanted phenomena, such as variation in flow discharge.

(b) Boundary layer developed from the bottom

In October of 1965, observation of boundary layer turbulence was conducted at Fukakusa point in the Sosui canal with a miniature propeller-type current meter. The canal has a regular trapezoidal cross section, which is shown in Fig. 6. 2. The side wall are made of stone masonry and the bottom is sandy. The stable turbulent boundary layer was expected to exist, because the upper reach of the canal from the observation point was straight for a distance of about 200 m. During the observation, the discharge of flow was 16 ton/sec and the slope of the canal was 1/4,000. A steel pipe 3 cm in diameter was used to support the current meter at various depths along the dotted line in Fig. 6. 2. Location of observation presented by a dotted line in this figure was too near to the side wall for the purpose of this section. In the following analyses of data, sampling duration and averaging time are uniformly 3 min and 1 sec, respectively.

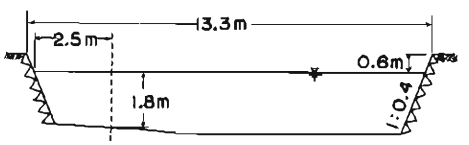

Fig. 6. 2 Cross-section of the Sosui canal at the observation station Fukakusa.

Mean velocity profile

The variation of the local temporal mean velocity $\bar{u}$ with height from the bottom is represented in Fig. 6. 3. The velocity profile was very nearly logarithmic throughout the vertical direction, and this made it possible to estimate the value of friction velocity u_* from the following expression,

$$u_*=\kappa\ d\bar{u}(z)/\mathrm{dlog}z, \qquad (6\cdot 2)$$

where κ is Karman's constant of 0.4[19]. The calculated friction velocity u_* was 5.4 cm/sec, which was 30 dyn/cm^2 in shearing stress. An estimate of u_* from $\sqrt{gRi}$ gives 4.2 cm/sec, where g is the acceleration of

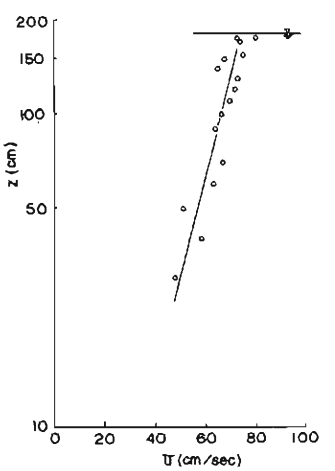

Fig. 6. 3 Logarithmic plot of mean velocity distribution in canal. Water depth $H=180$cm, friction velocity $u_*=5.4$ cm/sec, roughness length $z_0=0.7$cm, Reynolds number $Re=1.2\times 10^6$.

gravity, R the hydraulic radius and i the slope. Roughness was calculated as 0.7cm, which seems to be too great for the roughness of sand at first sight, but this value will be assumed to come from the roughness of the sand waves formed on the bottom. A drop of the point of maximum mean velocity was not observed. Average velocity along this measuring line U was 65 cm/sec and the Reynolds number calculated from this mean velocity and the depth UH/ν was 1.2×10^6. During the observation, a gentle wind was blowing against the water flow but the effect on the turbulence structure of the water flow was assumed to be negligible.

Intensity of turbulence

Vertical distribution of intensity of turbulence $\sigma_u/\bar{u}$ is presented in Fig. 6. 4. This result is compared with that of a number of measurements in the wind tunnel[20], atmospheric turbulence[1] and measurement in the tidal channel with an electromagnetic flowmeter[21] and that in a small size laboratory flume[2),4]. The tendency of distribution well agrees with that cited above but each value is rather high. The large value of intensities is supposed to come from numerous kinds of suspended matter in the flow, from the consideration of a study of a flow with a suspended load[22].

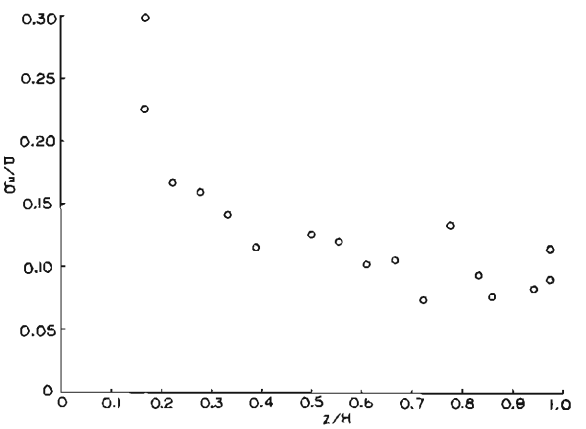

Fig. 6. 4. Relative turbulence intensity in a canal flow.

Eulerian correlation

Eulerian correlation coefficients were calculated by Eq. (3·3) at various depth. Representative curves in the upper, middle and lower parts of the flow are shown in Fig. 6. 5. The figure shows that as an increase of the height, correlation, that is, a time scale of turbulence becomes gradually larger. The time scale of the turbulence is represented quantitatively by the integral time scale,

$$T_x=\int_0^\infty R_x(t)\,dt. \tag{6·3}$$

This scale is generally difficult to determine because correlations do not come to zero at small lags. Semiscales were used, which were difined as the lag distances

at which the various correlations dropped to 0.60. If the correlation functions were exponential, the semiscales would be half the integral time scales of turbulence. The integral scale or mean eddy size in the longitudinal direction is then obtained using the assumption of frozen turbulence

$$L_x = \bar{u} T_x , \tag{6·4}$$

where T_x is twice the semiscale. The dependence of L_x on height which is linear increase is shown in Fig. 6. 6. In this observation, turbulence intensity may be somewhat large to permit the assumption of frozen turbulence. Longitudinal eddy viscisity was also estimated by the method of Taylor-Sutton

$$K_x = \overline{u'^2} T_x , \tag{6·5}$$

which is shown in Fig. 6. 7. There exist no appreciable variations of K_x with height except in the neighbourhood of the bottom, which well agrees with the Yudin-Shvets assumption[28],

$$K(z) \simeq \begin{cases} cz & \text{for } z < h \\ ch = K_h & \text{for } z > h , \end{cases} \tag{6·6}$$

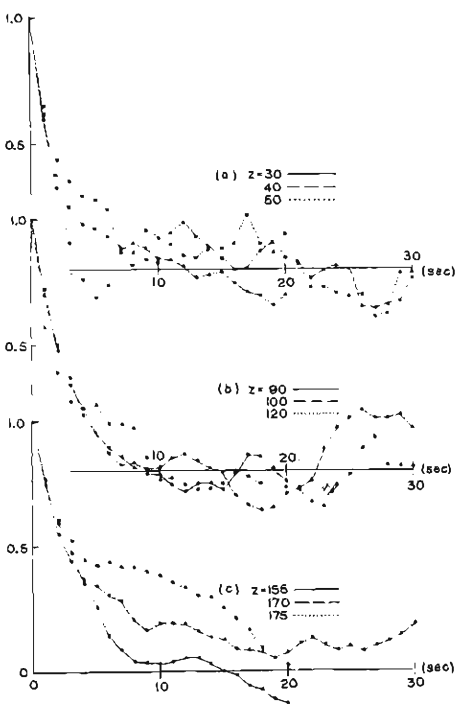

Fig. 6. 5 Autocorrelogram of longitudinal velocity fluctuations for different heights.

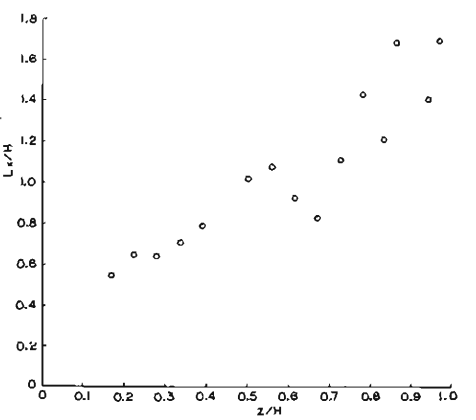

Fig. 6. 6 Dependence of longitudinal integral scale of turbulence on height. $H=180$cm.

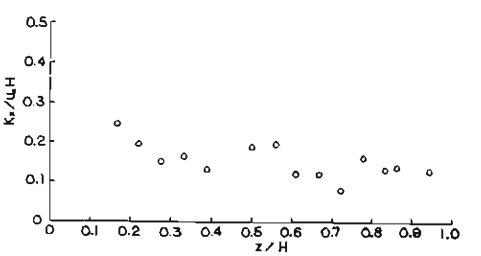

Fig. 6. 7 Dependence of longitudinal eddy viscosity on height. $u_*=5.4$cm/sec, $H=180$cm.

where c is some constant related to the friction velocity u_*. The value of K_x near the surface, $1.5\times10^2\,cm^2/sec$, agrees with an estimation by Richardson's 4/3 power law of diffusion[24].

Energy dissipation

The rate of dissipation of turbulent energy ε is one of the most important characteristics of turbulence and completely determines the motion in the inertial subrange of the spectrum. It was evaluated from the relationships

$$\varepsilon=\alpha\frac{u_0^3}{l_0}, \tag{6·7}$$

in which the constant α is determined by the choice of velocity and length scales. In this case we can set $\alpha=1$ to estimate the relative variation of these values. For the velocity scale u_0 we used the root mean square value of the longitudinal turbulent velocity $\sqrt{\overline{u'^2}}$ and for the length scale l_o the integral scale of turbulence L_x of the longitudinal component. The values of ε were made the nondimensional form with $\varepsilon_0=Ugi$, where U is an averaged velocity along the measuring line, g the acceleration of gravity and i the slope. The results of $\varepsilon/\varepsilon_0$ evaluations are given in Fig. 6. 8, which display a general tendency for the rate of dissipation to diminish sharply with depth[25].

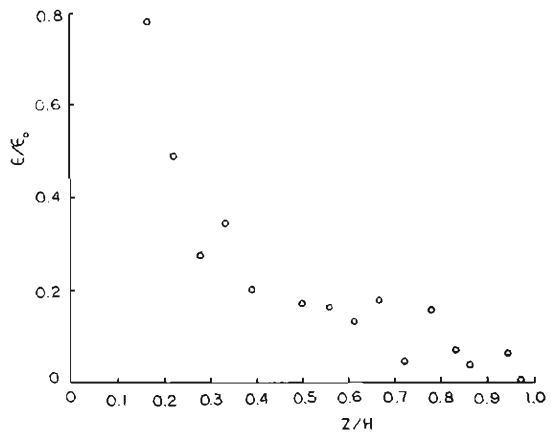

Fig. 6. 8 Vertical distribution of turbulent energy dissipation.

Power spectra

Normalized power spectra were calculated by Tukey's method (3·4). Representative curves are shown in Fig. 6. 9 like the correlations. Abscissa is in unit of $nz/\bar{u}$ (ratio of height to wavelength). Numerals in the graph indicate the height z in cm. The Kolmogorov $-5/3$ power law in the inertial subrange is not seen in the figure but a tendency of -1 power which was observed in the region close to the wall is seen[20]. The length of the largest eddies is supposed to be of the order of 10 times the height as mentioned in section 3, because the spectra seem to have their maximum values near the frequency $nz/\bar{u}=0.08$.

(c) Corner region between a side wall and free surface

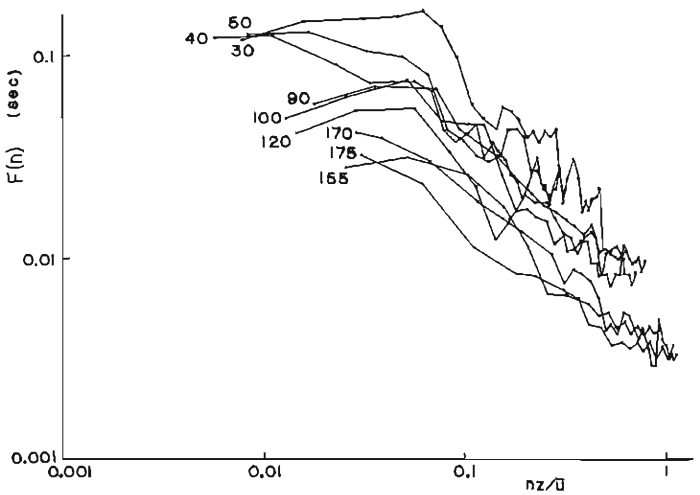

Fig. 6. 9 Normalized power spectra of longitudinal velocity at different heights as function of nondimensional frequency $nz/\bar{u}$.

For fully developed turbulent flow in a channel, there exists a transverse mean flow superimposed upon the longitudinal mean flow. This transverse flow, commonly known as secondary flow, interacts with the longitudinal mean flow and turbulence structure in a complex manner. Several detailed experiments have been conducted in a steady, incompressible, fully developed turbulent air flow in rectangular and triangular ducts[26),27)]. However there is no information about turbulence structure in the intersection region of a free surface and side wall.

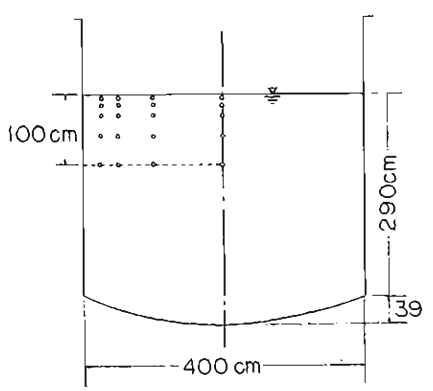

Fig. 6. 10 Cross-section of the Sosui canal at the observation point Shinomiya.

Measurements of turbulent velocity in the intersection region were conducted at Shinomiya in the Sosui canal with the miniature propeller-type current meter. The canal is covered with concrete and is 4 m in width, as shown in Fig. 6. 10. The slope of the canal was 1/2200, and Manning's coefficient of roughness was 0.019. During the observation, the water depth was 3m, discharge was 17.1 ton/sec, and mean velocity calculated from the discharge was 135 cm/sec. Therefore the Reynolds number with a hydraulic depth was about 2×10^6. The upper reach of the canal from the observation section was straight for a distance of about 110m, which made it possible to measure the stable fully developed boundary layer turbulence. The current meter was supported by a steel pipe 3 cm in diameter mounted on a bridge laid over the observation section. Velocity measurements were made at the points indicated in Fig. 6. 10. Duration of observation was

4 min and averaging time was 1 sec at each point.

Isovel patterns of longitudinal mean velocity are shown in Fig. 6. 11, which are made in nondimensional form divided by a cross-sectional mean velocity $U=$ 135 cm/sec. The distortion of the isovels in the corner region is clearly evident. Supposed secondary flows towards a corner are presented in this figure. The circulation on the free surface side seems to be flatter than that on the wall side. This secondary flow convects main flow momentum and energy towards the corner region,and is assumed to be the result of forces exerted by static pressure gradients and the Reynolds stresses in planes normal to the longitudinal direction[27]. Fig. 6. 12 shows the distribution of longitudinal turbulence intensity $\sigma_u/\bar{u}$. Intensity is very small near the free surface. Fig. 6. 13 shows the distribution of integral scale L_x, which was calculated from the integral time scale and frozen turbulence hypothesis. There exists a local maximum of mean eddy size in the corner region, which was not previously expected. Fig. 6. 14 shows the distribution of longitudinal eddy viscosity calculated from the root mean square value of turbulent velocity and integral time scale. The local maximum also exists in the corner region.

These preliminary experiments show the significant effect of a free surface on the turbulence structure of an open channel flow. More detailed measurements especially of Reynolds stress with an ultrasonic flowmeter are expected.

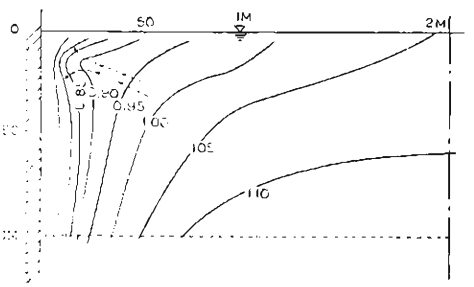

Fig. 6. 11 Isovel pattern of longitudinal mean velocity. Numerals give the value $\bar{u}/U$.

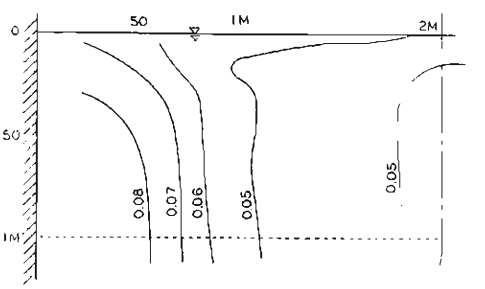

Fig. 6. 12 Lines of constant turbulence intensity.

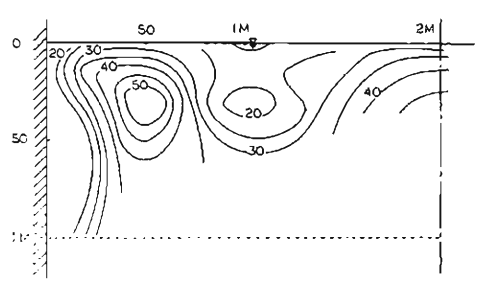

Fig. 6. 13 Distribution of longitudinal integral scale L_x (cm).

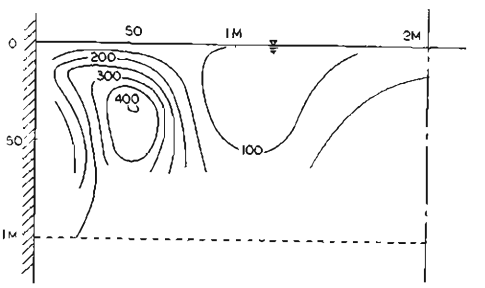

Fig. 6. 14 Distribution of longitudinal eddy viscosity K_x (cm²/sec).

7. Conclusion

River turbulence has many interesting properties of its own which are different from those in other fields of turbulence. In this paper, some of the properties were related to mean hydraulic parameters such as mean velocity, depth and width of flow. However, more detailed and extensive experiments are needed as a matter of curse. One of the most important and pressing matters for this purpose is to be sure of developing a suitable instrument for the measurements of river turbulence.

A propeller-type current meter is, as mentioned in this paper, very useful for the study of river turbulence. However, it has the fatal defects of impossibility of measuring the high frequency fluctuation of velocity and the velocity components perpendicular to the main flow. In the development of a new instrument possessing various items for measuring river turbulence, mere improvement of traditional measuring instruments will not be sufficient. Recently, many trial developments have been made on the basis of new principles, and an ultrasonic flowmeter is one of the remarkable instruments developed from them. The ultrasonic flowmeter even makes it possible to measure three components of velocity which are perpendicular to each other, simultaneously.

The ultrasonic flowmeter based on the method of sing-around has been used in our laboratory for the measurements of river turbulence. Simultaneous measurement of two components of velocity fluctuation is possible with this flowmeter. Furthermore, another type of ultrasonic flowmeter based on the method of pulse-time difference is being manufactured. A combination of these two ultrasonic flowmeters will make it possible to obtain the three-dimensional spectral density of turbulent velocity.

Acknowledgements

The author wishes to express his gratitude to professor Yasuo Ishihara for his useful discussions and encouragement throughout this work. The numerical computations were carried out by the KDC-I and KDC-II computers of Kyoto University Computer Center.

References

1) Lumley, J. L., and H. A. Panofsky (1964). The structure of atmospheric turbulence, 239 pp. Interscience.
2) Jonsson, I. G. (1965). On turbulence in open channel flow, Acta Polytechnica Scandinavica, Civil Engg. and Building Construction Series, No. 31.
3) Bowden, K. F. and J. Proudman, F. R. S. (1949). Observations on the turbulent fluctuations of a tidal current, Proc. Roy. Soc. A119, 311-327.
4) Raichlen, F. (1967). Some turbulence measurements in water, J. Engg. Mech. Division, Proc. ASCE, 93, 73-97.
5) Grant, H. L., R. W. Stewart and A. Moilliet (1962). Turbulence spectra from a tidal channel, J. Fluid Mech., 12, 241-268.
6) Bowden, K. F. and L. A. Fairbairn (1956). Measurements of turbulent fluctuations and Reynolds stresses in a tidal current, Proc. Roy. Soc. A237, 422-438.
7) Ishihara, Y. and S. Yokosi (1967). Observation of river turbulence with an ultrasonic flowmeter, Proc. 11 th Conf. Hydraulics in Japan, 53-58.

8) Kolmogorov, A. N. (1962). A refinement of previous hypotheses concerning the local structure of turbulence in a viscous incompressible fluid at high Reynolds number, J. Fluid Mech. 13, 82–85.
9) Kinoshita, R. (1967). An analysis of the movement of flood waters by aerial photography, concerning characteristics of turbulence and surface flow, Photographic surveying, 6, 1–17.
10) Ozmidov, R. V. (1965). Energy distribution between oceanic motions of different scales, Izv., Atmosph. and Oceanic Phys. Series, 1, 439–448.
11) Kolesnikova, V. N. and A. S. Monin (1965). Spectra of meteorological field fluctuations, Izv., Atmosph. and Oceanic Phys. Series, 1, 653–669.
12) Kraichnan, R. H. (1966). Isotropic turbulence and inertial-range structure, Phys. Fluid, 9, 1728–1752.
13) Blackman, R. B. and J. W. Tukey (1958). The measurement of power spectra, Dover.
14) Pasquill, F. (1962). Atmospheric diffusion, Van Nostrand, 297 pp.
15) Yokosi, S. (1966). Observation of turbulence in Sosui canal, Ann. Disaster Prevention Research Institute, 9, 513–523.
16) MacCready, P. B. (1962). The inertial subrange of atmospheric turbulence, J. Geophys. Research, 67, 1051–1059.
17) Townsend, A. A. (1956). The structure of turbulent shear flow, Cambridge U. P., 315 pp.
18) Yokosi, S. (1967). Large scale turbulence in a river, Ann. Disaster Prevention Research Institute, 10, 199-206.
19) Yokosi, S. and M. Kadoya (1965). Direct measurement of bottom shear stresses in open channel flows, Bulletin of the Disaster Prevention Research Institute, 15. 41–51.
20) Hinze, J. O. (1959). Turbulence, McGraw-Hill, 586 pp.
21) Bowden, K. F. and M. R. Howe (1963). Observations of turbulence in a tidal current. J. Fluid Mech., 17, 271–284.
22) Elata, C. and A. T. Ippen (1961). The dynamics of open channel flow with suspensions of neutrally buoyant particles. Tech. Report No. 45, Hydrodynamics Lab., MIT.
23) Byzova, I. L. (1964). The Yudin-Shvets formula for the boundary layer of the atmosphere with the application of similarity methods. Izv., Acad. Sci. USSR, Geophys. Ser., No. 8, 772–775.
24) Gunnerson, C. G. (1961). Discussion for "Eddy diffusion in homogeneous turbulence". Trans. ASCE, 126, 428.
25) Ivanov, V. N. (1962). Turbulent energy dissipation in the atmosphere. Izv., Acad. Sci. USSR, Geophys. Ser. 788.
26) Brundrett, E. and Baines, W. D. (1964). The production and diffusion of vorticity in duct flow. J. Fluid Mech. 19, 375–394.
27) Gessner, F. B. and J. B. Jones (1965). On some aspects of fully-developed flow in rectangular channels. J. Fluid Mech., 23, 689–713.